Computers and Structures xxx (2014) xxx–xxx

Contents lists available at ScienceDirect

Computers and Structures

journal homepage: www.elsevier.com/locate/compstruc

Definition of warping modes within the context of a higher order thin-walled beam model

R.F. Vieira *, F.B.E. Virtuoso, E.B.R. Pereira

Universidade de Lisboa, Instituto Superior Técnico, Department of Civil Engineering, Architecture and Georesources, Av. Rovisco Pais, 1049-001 Lisboa, Portugal

ARTICLE INFO

Article history:
Accepted 1 October 2014
Available online xxxx

Keywords:
Thin-walled structures
Higher order beam model
Warping modes

ABSTRACT

A procedure for the definition of uncoupled warping modes within the framework of a higher order beam model is presented. An approximation of the displacement field over the cross-section by a set of linearly independent basis functions is considered in the models formulation so as to capture 3D structural phenomena. By considering the cross-section in-plane rigid, a linear eigenvalue problem stemming from the models governing equations is derived, allowing to retrieve classic solutions and to derive a set of hierarchical warping modes. Numerical examples are presented in order to verify the ability of the model to simulate the warping of thin-walled structures.

1. Introduction

The structural analysis of thin-walled prismatic structures through one-dimensional models requires the consideration of higher order deformation modes in order to accurately represent its three dimensional structural behaviour. In fact, being those models derived by reducing the three-dimensional elasticity equations to a set of equations defined along the member axis by an appropriate projection of the displacement field, the definition of a convenient set of basis functions is essential to capture the 3D structural behaviour.

The warping of thin-walled structures with open cross-sections was considered by [1] through the definition of an additional coordinate for the approximation of the displacement field, the so-called sectorial coordinate. The cross-section was assumed to be in-plane undeformable and the shear deformation of the middle surface was neglected. A theory for the non-uniform torsion of closed cross-section was derived in [2,3], considering the shear strain of the cross-section midline to be given by the *Saint-Venant* uniform torsion theory. A more accurate theory for the non-uniform torsion of closed thin-walled beams was derived in [4,5] by considering an additional term representing the cross-section warping, which has an amplitude variable along the beam axis that is not related with the cross-section angle of torsion; reference should be made that this approach was also considered in [1] for solid sections. This theory is established and known as Benscoter theory, [6]. The cross-section "classic" warping is made orthogonal to the flexural modes by considering an adequate position for measuring the sectorial coordinate that defines the warping function, which is similar to consider the beam flexure around the principal axes in order to uncouple the axial force and bending moments.

A general theory for the analysis of thin-walled beams applied to a cross-section either with an open, closed or branched midline profile was presented in [7–9]. The theory relies on the assumption of the *Vlassov* hypothesis, considering only the shear strain corresponding to the theory of torsion by *Saint-Venant* for closed cross-section, [3]. The displacement field is approximated in terms of the derivative of its tangential components along the beam axis, being the axial displacements obtained through the hypothesis of neglecting the membrane shear strain, corresponding to a procedure already adopted by [10]. However, an orthogonality criterion similar to the classic warping was not possible to derive; instead, an uncoupling procedure based on an attempt do diagonalize the beam governing equations through generalised eigenvalue problems was adopted. A development of thin-walled beam models to the analysis of bridge structures considering warping modes was presented in [11–13], considering some of the formulations reported in [14] that follow the seminal work of [7–9,15].

The generalised beam theory (GBT) developed by [16,17] allows the definition of the cross-section deformation field through a cross-section discretization in terms of axial displacements, obtaining the transverse displacement by neglecting the shear strain. GBT was extended so as to consider (i) the shear-lag effect by adopting a set of shear-lag warping modes, [15,18], and (ii) the application to cross-sections with a generic midline profile geometry; recall that the initial formulation of GBT was developed for open cross-sections. Recently, further developments of the theory were made,

* Corresponding author.
E-mail address: ricardo.figueiredo.vieira@tecnico.ulisboa.pt (R.F. Vieira).

http://dx.doi.org/10.1016/j.compstruc.2014.10.005
0045-7949/

allowing its application to cross-sections with an open, closed or branched geometry, [19–22]. Regarding the uncoupling between deformation modes, the theory considers the diagonalization of the beam governing equations as a criteria, adopting towards this end a set of justified generalised eigenvalues problems.

Several other beam formulations accounting for the warping of thin-walled structures have been developed. Although, some of them were developed towards the application to specific structural behaviours, it is worth to mention some of the respective concepts.

A thin-walled beam formulation for anisotropic materials considering the out of plane warping of beam cross-sections but assuming its in-plane rigidity was presented by [23]. In that formulation, a set of orthogonal functions for the shear dependent warping of thin-walled beams was derived, being defined the corresponding weak form of the equilibrium equations. A set of orthogonal warping functions, defining the so-called *eigenwarpings*, were obtained from the solution of a generalised eigenvalue problem associated with the equilibrium differential equations. An "improved Bernoulli model" and an "improved Saint-Venant model" have been defined by adding to the Bernoulli model (linear axial displacement) and to the Saint-Venant model (linear axial stress distribution) a series expansion of these eigenwarpings.

The warping of thin-walled beams was also taken in account in [24] by considering an approximation of the thin-walled axial displacement field through a linear combination of basis functions only dependent of the cross-section coordinate. The basis functions are considered to be orthogonal to the uniform and linear functions associated with the translation and rotation of the cross-section. Comparatively to the model of [23], the formulation of [24] derives the system of governing equations from the assumptions made on the complete description of the displacement field, whereas in [23] the solution of warping is obtained separately for a specific displacement interpolation.

A thin-walled beam model applicable to cross-sections with both open and closed midline profiles, considering the cross-section in-plane rigid but including the membrane shear deformation, was presented in [25]. A shear flexible element considering warping was presented by [26], being the model applicable to thin-walled beams with an open profile of an arbitrary geometry. In terms of kinematics, the formulation considers the axial displacements of the cross-section to be defined through the linear combination of the axial displacement of the centroid, the cross-section rotations due to the flexure and the warping function defined through the sectorial coordinate. A finite element is derived considering the approximation of the displacement, rotation and warping through linear, quadratic and cubic functions, respectively.

A formulation for the analysis of thin-walled rectangular hollowed cross-sections subjected to torsion is developed in [27] in the sequel of a previous work, [28]. A set of orthogonal basis functions is adopted for the axial displacement of the cross-section webs, being the displacement of the flanges obtained from compatibility requirements. An equilibrium equation governing the warping of the walls is established in terms of the basis functions coordinates, which is proven to be independent of the angle of twist. On the other hand, an equation similar to the non-uniform torsion theory is derived, being the angle of twist coupled with the warping functions parameters.

A procedure for the definition of warping functions was presented in[29–32] within the framework of a beam model formulation. The beam model considers a division of the cross-section into rectilinear elements, being adopted a linear variation of the displacements along each wall element. The axial displacements are obtained adding to the Bernoulli displacements a linear combination of these additional warpings.

A thin-walled beam model that assumes the cross-section in-plane rigid but considers the out-of-plane warping and the "membrane" shear deformation is presented in this paper. The classic equations are retrieved side by side with a set of governing equations representing higher order deformations. In a previous work by the authors, [33], the warping modes were obtained from the solution of the quadratic eigenvalue problem associated with the differential equations of the beam model. In the sequel of a work presented by the authors in [34], an efficient, simple and innovative procedure for the definition of higher order warping modes is herein presented, being verified that these modes allow to accurately represent the higher order warping of in-plane deformable cross-sections. Towards the definition of orthogonal warping modes, the higher order beam model differential equations are rewritten in terms of axial displacements by considering the cross-section in-plane rigid, allowing to obtain a set of uncoupled warping modes directly from the corresponding linear symmetric eigenvalue problem. These modes are uncoupled according to bi-orthogonality conditions associated with linear symmetric eigenvalue problems, which allow to separate the structural phenomena of thin-walled structures. A comparison with the results of a higher order beam theory proposed by [35], which identifies similar warping modes but for an in-plane deformable cross-section, was successfully performed.

2. Model formulation

A one dimensional model for the analysis of thin-walled beams in order to consider the corresponding out-of-plane warping is developed. The formulation considers the cross-section to be in-plane rigid and includes the corresponding shear deformation. Towards an efficient approximation of the displacement field, the cross-section is divided into laminar elements, being the displacement field approximated for each element along the corresponding middle surface (see Fig. 1).

2.1. Displacement field

The displacement field is defined admitting the beam cross-section to be "divided" into n laminar elements without any geometrical restriction, i.e., it is possible to deal with more than two walls converging in a node as well as to consider two consecutive aligned walls. The displacement components are defined through a set of interpolation functions independently of the corresponding direction. A local reference frame $O(x,s,n)$ is adopted, being the beam longitudinal axis represented by x, whereas n represents the perpendicular direction relatively to the wall and s the running coordinate along the cross-section midline profile. The middle surface is therefore defined by the cartesian pair (x,s). A cross-section discretization is represented in Fig. 2.

The structural behaviour of the thin-walled beam is reduced to the cross-section midline profile considering only the corresponding membrane behaviour inasmuch as the cross-section in-plane deformation is disregarded and hence the plate behaviour of the wall is neglected. The displacement field is defined as follows:

$$u_x(x,s,n) = \tilde{u}_x(x,s) = \mathbf{\Phi}\,\mathbf{u}_x \quad \text{and} \quad u_s(x,s,n) = \tilde{u}_s(x,s) = \mathbf{\Psi}\,\mathbf{u}_s \tag{1}$$

where $\mathbf{\Phi}$ and $\mathbf{\Psi}$ represent the arrays grouping the corresponding interpolation functions, being $\tilde{u}_x$ and $\tilde{u}_s$ the respective amplitudes. A set of p and m linear independent approximation functions is considered:

$$\mathbf{\Phi} = [\phi_1, \ldots, \phi_p] \quad \text{and} \quad \mathbf{\Psi} = [\psi_1, \ldots, \psi_m] \tag{2}$$

being the respective amplitudes given by:

$$\mathbf{u}_x = [u_{x1}, \ldots, u_{xp}]^t \quad \text{and} \quad \mathbf{u}_s = [u_{s1}, \ldots, u_{sm}]^t \tag{3}$$

Please cite this article in press as: Vieira RF et al. Definition of warping modes within the context of a higher order thin-walled beam model. Comput Struct (2014), http://dx.doi.org/10.1016/j.compstruc.2014.10.005

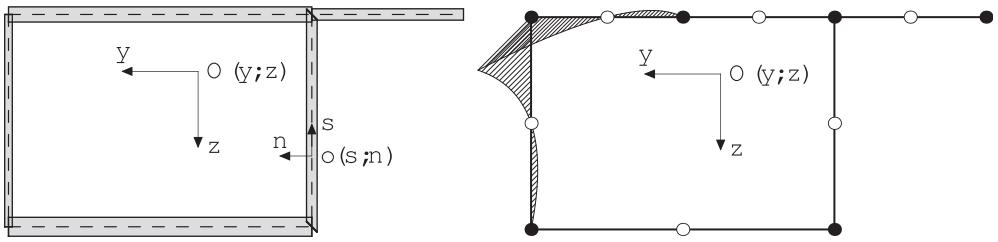

Fig. 1. Cross-section discretization.

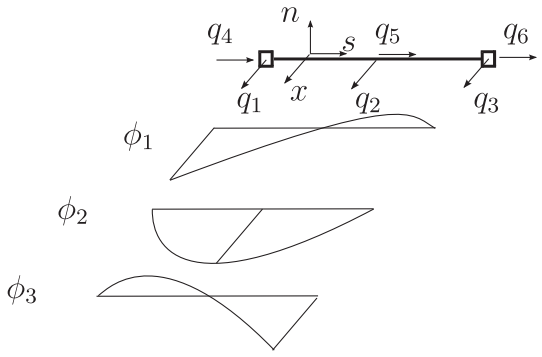

Fig. 2. Approximation functions for a cross-section element.

2.2. Deformation field

The deformation field represents the thin-wall membrane structural behaviour, being obtained by assuming the small displacement hypothesis through the following expressions:

$$\epsilon_x(x,s) = \frac{\partial \tilde{u}_x}{\partial x} \tag{4}$$

$$\epsilon_s(x,s) = \frac{\partial \tilde{u}_s}{\partial s} \tag{5}$$

$$\gamma_{xs}(x,s) = \frac{\partial \tilde{u}_x}{\partial s} + \frac{\partial \tilde{u}_s}{\partial x} \tag{6}$$

By substituting the approximations defined in (1), the deformation field can be rewritten in a more compact form as follows,

$$\boldsymbol{\epsilon} = \mathbf{E}\mathbf{e} \tag{7}$$

being $\mathbf{E}$ and $\mathbf{e}$ defined by

$$\mathbf{E} = [\mathbf{E}_1, \mathbf{E}_0], \quad \mathbf{e} = [\mathbf{u}', \mathbf{u}]^t \tag{8}$$

with

$$\mathbf{u} = [\mathbf{u}_x, \mathbf{u}_s], \quad \mathbf{E}_0 = \begin{bmatrix} \cdot & \cdot \\ \cdot & \boldsymbol{\Psi}_{,s} \\ \boldsymbol{\Phi}_{,s} & \cdot \end{bmatrix} \quad \text{and} \quad \mathbf{E}_1 = \begin{bmatrix} \boldsymbol{\Phi} & \cdot \\ \cdot & \cdot \\ \cdot & \boldsymbol{\Psi} \end{bmatrix} \tag{9}$$

where: (i) the matrix $\mathbf{E}$ groups the cross-section deformation modes, (ii) the vector $\mathbf{e}$ represents the corresponding parameters and (iii) the vector $\mathbf{u}$ corresponds to the amplitudes of the displacement field approximations over the cross-section. The compatibility conditions are written as follows,

$$\mathbf{e} = \mathbb{D}^* \mathbf{u} \tag{10}$$

being $\mathbb{D}^*$ a compatibility differential operator defined by

$$\mathbb{D}^* = \begin{bmatrix} \boldsymbol{\partial}_x^* \\ \mathbf{I} \end{bmatrix} \quad \text{with} \quad \boldsymbol{\partial}_x^* = \begin{bmatrix} \frac{d}{dx} & & \\ & \ddots & \\ & & \frac{d}{dx} \end{bmatrix} \tag{11}$$

2.3. Constitutive relations

A linear, elastic and isotropic behaviour is admitted for each thin-walled element, being considered the following constitutive relation,

$$\boldsymbol{\sigma} = \mathbf{C}\boldsymbol{\epsilon} \quad \text{with} \quad \mathbf{C} = \begin{bmatrix} E^* & E^* v & \cdot \\ E^* v & E^* & \cdot \\ \cdot & \cdot & G \end{bmatrix} \tag{12}$$

where G represents the distortion *moduli* and E^* represents the elastic *moduli* of a plane state of stress, being given through:

$$G = \frac{E}{2(1+v)} \quad \text{and} \quad E^* = \frac{E}{1-v^2} \tag{13}$$

It is convenient for the model formulation to have a "discrete" measure associated with the continuum variable that represents the stress field, $\boldsymbol{\sigma}$. This variable would be the dual variable in relation to the deformation parameters $\mathbf{e}$ defined in (8). Hence, a vector of generalised internal forces is defined by weighting the stress field through the deformation modes as follows,

$$\mathbf{s} = \int_A \mathbf{E}^t \boldsymbol{\sigma}\, dA \tag{14}$$

The vector $\mathbf{s}$ represents a set of generalised forces, including the classic internal forces from the classic beam theories and internal forces (self-equilibrated) of higher order. For the sake of consistency with the developed formulation these generalised forces are rewritten as follows,

$$\mathbf{s} = [\mathbf{s}_1, \mathbf{s}_0]^t \tag{15}$$

The relation between the generalised forces $\mathbf{s}$ and the corresponding deformation parameters is obtained by ensuring that the deformation energy of these discrete measures equals the energy associated with the corresponding continuum variables, namely the stress and deformation field. The following constitutive relation at a cross-section level is then obtained:

$$\mathbf{s} = \mathbf{K}\mathbf{e} \tag{16}$$

being the siffness matrix $\mathbf{K}$ defined as follows,

$$\mathbf{K} = \begin{bmatrix} \mathbf{K}_{11} & \mathbf{K}_{10} \\ \mathbf{K}_{01} & \mathbf{K}_{00} \end{bmatrix} \quad \text{and} \quad \mathbf{K}_{ij} = \int_A \mathbf{E}_i^t \mathbf{C} \mathbf{E}_j\, dA \quad \text{for} \quad i,j = 0,1,2 \tag{17}$$

2.4. Equilibrium equations

The equilibrium equations are obtained, assuming valid the small displacements hypothesis, through the dual relation of the compatibility conditions written in Eq. (10), being written as follows,

$$\mathbb{D}\mathbf{s} + \mathbf{p} = 0 \quad \text{with } \mathbb{D} = [\boldsymbol{\partial}_x, -\mathbf{I}] \tag{18}$$

Please cite this article in press as: Vieira RF et al. Definition of warping modes within the context of a higher order thin-walled beam model. Comput Struct (2014), http://dx.doi.org/10.1016/j.compstruc.2014.10.005

where (i) $\mathbb{D}$ represents the equilibrium differential operator, which is adjoint of the compatibility operator $\mathbb{D}^*$ and (ii) $\mathbf{p}$ represents the load vector. The equilibrium Eq. (18) represent the dual relation of the compatibility conditions written in (10).

The equilibrium equations can be written in terms of the amplitudes of the basis functions that approximate the displacement field over the cross-section by substituting in Eq. (18) the constitutive relations (16) and the compatibility conditions (10), which renders the following equation,

$$\mathbb{D}\,\mathbf{K}\,\mathbb{D}^*\,\mathbf{u}(x)+\mathbf{p}=0 \tag{19}$$

After performing the operations corresponding to the differential operators, the governing equation can be rewritten in the following format,

$$\mathbb{K}_2\mathbf{u}''(x)+\mathbb{K}_1\mathbf{u}'(x)+\mathbb{K}_0\mathbf{u}(x)=0 \tag{20}$$

where $(') = \frac{d}{dx}$ and the coefficient matrices are obtained as follows,

$$\mathbb{K}_2=\mathbf{K}_{11}=\int_A \mathbf{E}_1^t\,\mathbf{C}\,\mathbf{E}_1\,dA \tag{21}$$

$$\mathbb{K}_1=\mathbf{K}_{10}-\mathbf{K}_{01}^t=\int_A \left(\mathbf{E}_1^t\,\mathbf{C}\,\mathbf{E}_0-\mathbf{E}_0^t\,\mathbf{C}\,\mathbf{E}_1\right)dA \tag{22}$$

$$\mathbb{K}_0=\mathbf{K}_{00}=\int_A \mathbf{E}_0^t\,\mathbf{C}\,\mathbf{E}_0\,dA \tag{23}$$

Since the approximation functions are linear independent, the matrix $\mathbb{K}_2$ is verified to be non-singular. The matrix $\mathbb{K}_1$ has a skew-symmetric structure and the matrix $\mathbb{K}_0$ is symmetric and singular.

By considering the approximations of the displacement field defined in (1), the coefficient matrices defined in (21)–(23), can be written by diagonal blocks as follows,

$$\mathbb{K}_2=\begin{bmatrix}\mathbf{K}_{2,a} & \cdot\\ \cdot & \mathbf{K}_{2,t}\end{bmatrix},\quad \mathbb{K}_1=\begin{bmatrix}\cdot & \mathbf{K}_1\\ -\mathbf{K}_1^t & \cdot\end{bmatrix}\quad\text{and}\quad \mathbb{K}_0=\begin{bmatrix}\mathbf{K}_{0,a} & \cdot\\ \cdot & \mathbf{K}_{0,t}\end{bmatrix}$$

being the corresponding submatrices defined through:

$$\mathbf{K}_{2,a}=E^*t\int_A \mathbf{\Phi}\otimes\mathbf{\Phi}\,dA$$

$$\mathbf{K}_{2,t}=G\,t\int_A \mathbf{\Psi}\otimes\mathbf{\Psi}\,dA$$

$$\mathbf{K}_{0,a}=G\,t\int_A \mathbf{\Phi}_{,s}\otimes\mathbf{\Phi}_{,s}\,dA$$

$$\mathbf{K}_{0,t}=G\,t\int_A \mathbf{\Psi}_{,s}\otimes\mathbf{\Psi}_{,s}\,dA$$

$$\mathbf{K}_1=G\,t\int_A \mathbf{\Phi}_{,s}\otimes\mathbf{\Psi}\,dA$$

3. Uncoupling procedure

3.1. General concept

The successful application of a beam model to the analysis of the three-dimensional behaviour of thin-walled beams depends on the refinement considered for the displacement field projection, which can be obtained through an enrichment of the approximation functions or by a refinement of the corresponding mesh, (cross-section discretization). However, if the resulting governing equations are not properly uncoupled, the result is a tangled set of equations that although the fact of representing the elasticity formulation of the problem do not allow a clear physical interpretation of the structural phenomena.

Hence, the procedure of uncoupling the beam governing equations after a proper projection of the displacement field is mandatory. In this paper, a new concept of uncoupling is put forward by taking in account the eigenvalue statement associated with the beam equations homogeneous solution and also the particular case that neglects the cross in-plane deformability, which allows to simplify the problem and defines a systematic and simple procedure to obtain warping functions.

The conceptual idea of uncoupling within the framework of this beam model is to derive the corresponding set of displacement modes from a set of orthogonal solutions.

The beam differential equation is intimately associated with the quadratic eigenvalue problem. In fact, the general solution for Eq. (20) can be written in an exponential form as follows,

$$\mathbf{u}(x)=\mathbf{u}_0\,e^{(\lambda x)} \tag{24}$$

The substitution of the solution (24) into the beam model Eqs. (20) yields the following set of equations,

$$\mathbf{Q}(\lambda)\,\mathbf{u}_0\,e^{\lambda x}=0\quad\text{with}\quad \mathbf{Q}(\lambda)=\mathbb{K}_2\,\lambda^2+\mathbb{K}_1\,\lambda+\mathbb{K}_0 \tag{25}$$

which, since $e^{\lambda x}>0$, corresponds to the following set of algebraic equations,

$$\mathbf{Q}(\lambda)\,\mathbf{u}_0=0 \tag{26}$$

The Eq. (26) represents a quadratic eigenvalue problem, being λ and $\tilde{\mathbf{u}}_0$ the eigenvalue and the corresponding eigenvector, respectively. A reference should be made to the fact that the solution (24) was already considered by [36–38] for plane elasticity problems and by [39] for beams with a solid cross-section with a three-dimensional behaviour in order to provide a quantification for the *Saint-Venant* principle, being the exponent parameter λ identified as the inverse of a decay length associated with the solution.

The solution of the eigenvalue problem regarding the definition of the corresponding eigenvectors and eigenvalues and a transformation of coordinates that guarantee the same spectrum (set of eigenvalues) is not as simple and straightforward as in the case of the standard eigenvalue problem. A major difference in relation to the more usual eigenvalue problems, namely the standard and the generalised eigenvalue problems, is the fact that in the quadratic eigenvalue problem the number of eigenvalues to obtain is twice of the problem dimension, i.e., $(2\times n)$, and therefore the associated eigenvectors cannot form a linearly independent set of vectors. Hence, the definition of the eigenvectors for a new base of the equations is not possible.

Essentially two approaches exist regarding the quadratic eigenvalue problem solution: (i) one that considers the problem in its original form and seeks for a solvent of the corresponding set of algebraic equations and (ii) other that linearises the problem in order to obtain a solution through a generalised eigenvalue problem. The use of a linearisation is the usual procedure since it has a simple numerical implementation. However, careful must be taken in order to preserve the initial symmetric/skew-symmetric structure of the problem, otherwise a different structural phenomena is being considered.

The structure of the eigenvalue problem, i.e. the symmetry of $\mathbb{K}_2$ and $\mathbb{K}_0$ and the skew symmetry of $\mathbb{K}_1$, implies a spectrum symmetric not only in relation to the real axis but also symmetric in relation to the imaginary axis, [40]. Therefore, if λ is an eigenvalue of the problem so are the eigenvalues $-\lambda, \bar{\lambda}$ and $-\bar{\lambda}$. The linear form of the beam quadratic eigenvalue problem should therefore reproduce such spectrum location. However, one of the most common linearisations in differential equations corresponds to consider the following system of equations,

$$\mathbf{A}\tilde{\mathbf{w}}'-\mathbf{B}\tilde{\mathbf{w}}=\mathbf{0}\quad\text{with}\quad \tilde{\mathbf{w}}=[\,\mathbf{u}'(x)\quad\mathbf{u}(x)\,]^t \tag{27}$$

being the coefficient matrices $\mathbf{A}$ and $\mathbf{B}$ square matrices of dimension $2n$ (doubling the problem dimension) given through,

$$\mathbf{A} = \begin{bmatrix} \mathbb{K}_2 & \cdot \\ \cdot & \mathbf{I} \end{bmatrix} \quad \text{and} \quad \mathbf{B} = \begin{bmatrix} \mathbb{K}_1 & \mathbb{K}_0 \\ \mathbf{I} & \cdot \end{bmatrix} \tag{28}$$

However, both matrices presented in (27) are neither Hamiltonian nor skew-Hamiltonian and hence the spectrum symmetry will not be preserved. In fact,

$$(\mathbf{AJ})^t \neq \mathbf{AJ} \quad \text{with} \quad \mathbf{J} = \begin{bmatrix} \cdot & \mathbf{I} \\ -\mathbf{I} & \cdot \end{bmatrix} \tag{29}$$

Therefore, and in order to preserve the symmetric structure of the problem, the symmetric linearisation of the beam differential equation adopted for this formulation yields the following associated generalised eigenvalue problem,

$$\begin{aligned} &(\bar{\mathbf{B}} - \lambda \bar{\mathbf{A}})\tilde{\mathbf{w}}_0 = 0 \\ &\bar{\mathbf{A}} = \begin{bmatrix} \cdot & -\mathbb{K}_0 \\ \mathbb{K}_2 & \cdot \end{bmatrix} \quad \bar{\mathbf{B}} = \begin{bmatrix} \mathbb{K}_2 & \mathbb{K}_1 \\ \cdot & \mathbb{K}_2 \end{bmatrix} \end{aligned} \tag{30}$$

In fact, these matrices are respectively Hamiltonian, $\bar{\mathbf{A}}$ and skew-Hamiltonian $\bar{\mathbf{B}}$, which imply that the solution of the generalised eigenvalue problem allows to obtain a spectrum both symmetric to the real and imaginary axes.

The set of eigenvalues obtained from Eq. (26) for the beam governing equations assuming the cross-section in-plane rigid corresponds to pairs of symmetric real non-null values and a null eigenvalue representing a twelve fold root, i.e. with an algebraic multiplicity of 12. The symmetric values correspond to solutions decaying along both directions along the beam longitudinal axis, whereas the null eigenvalue corresponds to a polynomial solution with no decaying pattern.

3.2. Classic modes

The null eigenvalue is a twelve fold solution of Eq. (30), which corresponds to non-decaying solutions: six rigid body motions and the Saint Venant classic solutions of extension, flexure and uniform torsion. Hence, the 12 corresponding eigenvectors that would represent a basis for the displacement modes associated with those solutions have to be obtained. However, since the algebraic and the geometric multiplicities of the null eigenvalue do not coincide, a Jordan chain block of matrices has to be obtained in order to identify the respective generalised eigenvectors, [41].

This fact corresponds to consider for the beam governing equation a general solution of the following form,

$$\mathbf{u}(x) = \left(\frac{x^k}{k!}\mathbf{u}_0 + \cdots + \mathbf{u}_{k-1} + \mathbf{u}_k \right) e^{\lambda x} \quad \text{with } \tilde{\mathbf{u}}_0 \neq 0 \tag{31}$$

where in the absence of span loads $k = 3$. According to [42] the solution (31) is valid if and only if the following equalities holds,

$$\sum_{j=0}^{i} \frac{1}{j!}\mathbf{Q}^j(0)\,\mathbf{u}_{i-j} = 0 \quad \text{for} \quad i = 0 \ldots k \tag{32}$$

where the superscript j in $\mathbf{Q}^{(j)}(0)$ represents the j^{th} derivative in relation to λ of the matrix $\mathbf{Q}$. The application of (32) results in the successive solution of a linear system of equations. The first set of equations, corresponding to $j = 0$ and $i = 0$, reads as follows,

$$\mathbb{K}_0\,\mathbf{u}_0 = \mathbf{0} \tag{33}$$

being the solution obtained by the null space of matrix $\mathbb{K}_0$. The vectors $\mathbf{u}_0$ are eigenvectors associated with $\lambda_0 = 0$, spanning a space of dimension β_0, i.e., the geometric multiplicity of eigenvalue λ_0. Since $\beta_0 < \alpha = 12$ and providing that $\mathbf{u}_0 \neq \mathbf{0}$ the next set of equations needs to be considered. The following set of equations is then solved,

$$\mathbb{K}_0\,\mathbf{u}_0 = \mathbf{0} \quad \text{and} \quad \mathbb{K}_1\,\mathbf{u}_0 + \mathbb{K}_0\,\mathbf{u}_1 = \mathbf{0}$$

being mandatory that the eigenvector should not be null, i.e., $\mathbf{u}_0 \neq \mathbf{0}$. For the beam homogeneous differential equations it was verified that for achieving a convergence, i.e., $\beta = \alpha = 12$, four sets of equations are required, corresponding to 4 sets of generalised eigenvectors: $\mathbf{u}_0$, $\mathbf{u}_1$, $\mathbf{u}_2$, and $\mathbf{u}_3$.

3.3. Application to cross-sections rigid in-plane

The uncoupling procedure described in Section 3.1 that relies on the solution of a quadratic eigenvalue problem for the definition of orthogonal warping modes was adopted in [33]. However, for a cross-section considered in-plane rigid, a simpler and yet alternative procedure can be adopted for the definition of such warping modes.

A closer analysis of the differential beam governing equations allows to conclude that it is possible to establish a relation between the transverse displacement amplitudes and the amplitudes of the axial displacements approximation. This fact allows to write the beam governing equations exclusively in terms of the axial amplitudes, in a procedure similar to the dynamic analysis, which is well known as static condensation. Towards this end, considering the coefficient matrices defined in (24) and given the fact that since the in-plane cross-section deformation is neglected the submatrix $\mathbf{K}_{0,t}$ becomes null, the beam governing equations are separated in the axial direction and in the transverse direction as follows,

$$\mathbf{K}_{2,a}\mathbf{u}_a''(x) + \mathbf{K}_1\mathbf{u}_t'(x) - \mathbf{K}_{0,a}\mathbf{u}_a(x) = \mathbf{0} \tag{34}$$

$$\mathbf{K}_{2,t}\mathbf{u}_t''(x) - \mathbf{K}_1\mathbf{u}_a'(x) = \mathbf{0} \tag{35}$$

Given the fact that the sets of approximation functions, $\boldsymbol{\Phi}$ and $\boldsymbol{\Psi}$, are constituted by linear independent basis functions the submatrices $\mathbf{K}_{2,a}, \mathbf{K}_{2,a}$ are non-singular and hence can be inverted. Considering the Eq. (35), it is possible to obtain a relation between the axial and transverse amplitudes of the displacement approximation functions through the integration of Eq. (35),

$$\mathbf{u}_t'(x) = \mathbf{K}_{2,t}^{-1}\mathbf{K}_1\mathbf{u}_a(x) + \mathbf{c} \tag{36}$$

The subsequent substitution into the axial equilibrium equations allows to obtain a simplified governing differential system of equations,

$$\mathbf{K}_{2,a}\mathbf{u}_a''(x) - \mathbf{K}_{0,a}^{*}\mathbf{u}_a(x) = \mathbf{c}^{*} \tag{37}$$

being the matrix $\mathbf{K}_{0,a}$ defined by

$$\mathbf{K}_{0,a}^{*} = \left(\mathbf{K}_{0,a} - \mathbf{K}_1\mathbf{K}_{2,t}^{-1}\mathbf{K}_1\right)\mathbf{u}_a(x) \tag{38}$$

which is a symmetric matrix. Considering a general homogeneous solution of Eq. (37) given by:

$$\mathbf{u}_a(x) = \mathbf{u}_{a0}\, e^{\sqrt{\mu}x} \tag{39}$$

a generalised eigenvalue problem, allowing to obtain the warping modes for the beam cross-section is obtained,

$$\left(\mu\mathbf{K}_{2,a} - \mathbf{K}_{0,a}^{*}\right)\mathbf{u}_{a0} = 0 \tag{40}$$

The eigenvectors obtained by Eq. (40) allow to obtain a general homogeneous uncoupled solution of the beam governing equations for the higher order deformation modes, i.e., modes with a decaying behaviour along the beam axis.

4. Implementation of the beam model

The approximation of the displacement filed over the beam cross-section can be performed either in a global form or considering a discretization of the cross-section into rectilinear elements,

Please cite this article in press as: Vieira RF et al. Definition of warping modes within the context of a higher order thin-walled beam model. Comput Struct (2014), http://dx.doi.org/10.1016/j.compstruc.2014.10.005

being the displacement approximation performed over each element. The later procedure has the advantage of having a more efficient implementation as well as enhancing h refinement for the displacement approximation. The approximation of the axial displacements for the cross-section element considering quadratic functions is represented in Fig. 2.

The beam governing equations are obtained from the assembly of the coefficient matrices of the element equations by taking in account the compatibility between cross-section elements. However, the tangential deformability of each cross-section element is considered by this form. Since the cross-section in-plane deformability is not considered in this work, the cross-section transverse displacements are referred to the displacements of a generic point of the cross-section through a proper change of coordinates or alternatively a matrix of restrictions regarding the tangential relative displacement for each wall can be built.

The classic and warping modes are obtained for the beam governing equations through the procedures described in Sections 3.2 and 3.3. A change of coordinates for the beam equations is considered by a set of orthogonal displacement modes obtained from the generalised eigenvectors and eigenvectors, allowing to establish a set of "uncoupled" equilibrium equations; this set of equations can be written in terms of internal forces, allowing to recover the beam classic equilibrium equations and establish a similar set of equations in terms of generalised internal forces associated with warping modes.

A solution of the axial beam displacement is derived by taking in account the eigenvalues obtained through Eq. (40). The beam axial displacement can then be obtained as follows,

$$\mathbf{u}_a(x) = \alpha_1 \mathbf{u}_{a,1} e^{\mu_1 x} + \alpha_2 \mathbf{u}_{a,2} e^{\mu_2 x} \cdots \alpha_m \mathbf{u}_{a,m} e^{\mu_m x} \tag{41}$$

where $m \leqslant n$ because the null eigenvalues have an algebraic multiplicity. The constants α_i are obtained by taking in account the boundary conditions. However, a finite element procedure is adopted to solve the differential equations along the beam axis. Therefore, instead of considering the constants α_i together with the associated exponential form $e^{\mu_i x}$, a new variable dependent on the beam axis coordinate $\tilde{\alpha}_i(x)$ is introduced rewriting the beam displacements as follows,

$$\mathbf{u}_a(x) = \tilde{\alpha}_1(x)\mathbf{q}_{x1} + \tilde{\alpha}_2(x)\mathbf{q}_{x2} \cdots \tilde{\alpha}_m(x)\mathbf{q}_{xm} \tag{42}$$

where $\mathbf{q}_{x1}$ to $\mathbf{q}_{xm}$ correspond to the amplitudes of the interpolation functions along the beam axis for the warping deformation modes.

5. Examples of application

Some examples of thin-walled structures are analysed by the developed beam model so as to highlight (i) the adopted procedure for the definition of warping modes and (ii) the model's capability in representing the higher order effects regarding the out-of-plane warping of thin-walled structures. Warping modes of cross-sections with different profile geometries were obtained through the proposed uncoupling procedure. The local influence of higher order warping modes can be verified through the results obtained for the structural analysis of the structure in terms of stresses distributions along the beam axis, being identified a decaying pattern. The results obtained through the proposed model were compared with previous beam theories as well as with the results obtained from a shell finite element model implemented in [43], allowing to verify the accuracy of the model. Moreover, a comparison with a higher order beam theory presented in [35] that considers both transverse and warping eigenmodes was performed, verifying that the warping modes defined by considering the hypothesis of a cross-section in-plane rigid accurately represent membrane axial stresses of in-plane deformable cross-sections.

5.1. Identification of the cross-section warping modes

A thin-walled rectangular hollow section made of concrete is considered. The concrete behaviour is admitted to be linear, elastic and isotropic, with an elastic modulus of $E = 21$ GPa. In terms of the cross-section discretization, two solutions were analysed: (i) the cross-section divided into 6 "quadratic" elements (two elements for the flange and 1 element for the web) considering the axial displacements to be approximated through Lagrange quadratic functions and (ii) the cross-section divided into 12 "linear" elements (6 elements for each flange and two elements per web) adopting linear functions for the approximation of the axial displacement. The tangential displacement was approximated by linear functions in both discretisations.

The set of deformation modes was obtained from the uncoupling procedure described in 3.2 and 3.3 through a generalised eigenvalue problem. The eigenvalues obtained are real numbers and occur in symmetric pairs. A null eigenvalue with an algebraic multiplicity of 12 was obtained, which since the corresponding geometric multiplicity was different implies the computation of a Jordan chain of matrices. The Jordan matrices obtained allowed to identify the corresponding classic deformation modes as well as a warping associated with the shear deformation.

The higher order warping modes for the rectangular hollow section are represented in Figs. 3 and 4. The modes obtained from the two discretisations are presented: a linear approximation that considers the cross-section divided into 12 elements and a quadratic approximation with 6 elements. The modes are presented hierarchically according to the respective decay length; hence, the warping modes of Fig. 3 have a slower decay than the modes represented in Fig. 4. The higher order modes represented in Fig. (3) represent shear-lag modes, being associated with the corresponding flexure modes, whereas the modes in Fig. 4 represent a shear-lag mode associated with the extension (on the left side) and a higher order mode related to shear deformation of both flanges (on the right side).

A twin hollow cross-section obtained by introducing a sept into the previous rectangular hollow section was also analysed. For the approximation of the displacement field both quadratic and linear functions were adopted, namely a discretization into 7 quadratic elements (one per wall of each cell) and into 14 linear elements (two elements per wall of each cell, respectively).

A set of shear-lag warping modes is represented in Fig. 5 for the quadratic element approximation and for the linear approximation with 14 elements. The eigenvalues obtained for these modes through the two approximations solutions are similar. The discretization with 7 linear elements does not allow to capture such modes, being the corresponding eigenvalues higher and closer to the higher order warping modes represented in Fig. 6.

5.2. Beam analysis

A simple supported thin-walled structure with a twin cell hollow section is considered, in order to verify the use of the warping modes derived within the context of the higher order beam model that was presented. The structure represents a concrete girder spanning a length of $L = 15$ m. The beam cross-section is a twin cell hollow section with an overall width of $2b = 2$ m and a height of $h = 1$ m, having a constant thickness of $t = 0.15$ m. For the material an elastic *moduli* of $E = 21$ GPa with a *Poisson* coefficient of $v = 0.2$ was considered. The results are compared with a shell finite element implemented in [43]. This example was chosen since it was already performed in [7] and later in [19], allowing to establish a comparison between results.

The cross-section was discretised into 7 quadratic elements, being the warping modes defined according to the procedure in

Please cite this article in press as: Vieira RF et al. Definition of warping modes within the context of a higher order thin-walled beam model. Comput Struct (2014), http://dx.doi.org/10.1016/j.compstruc.2014.10.005

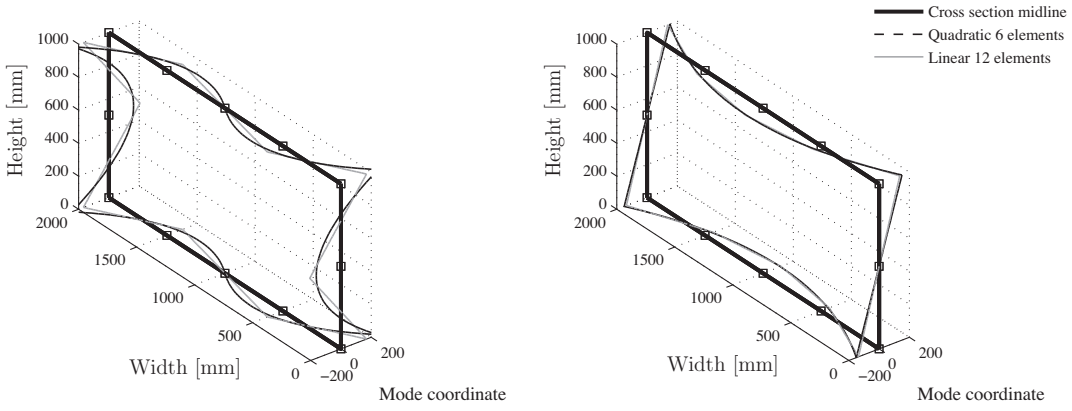

Fig. 3. Rectangular hollow section, 1st and 2nd warping modes.

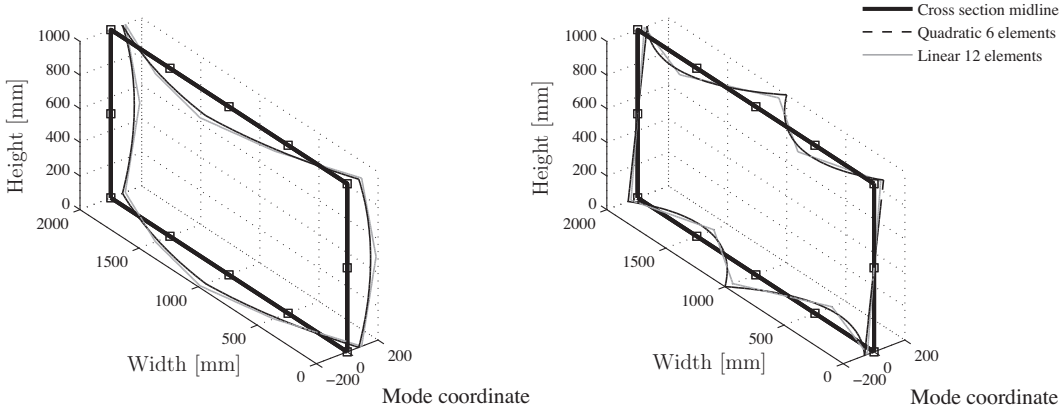

Fig. 4. Rectangular hollow section, 3rd and 4th warping modes.

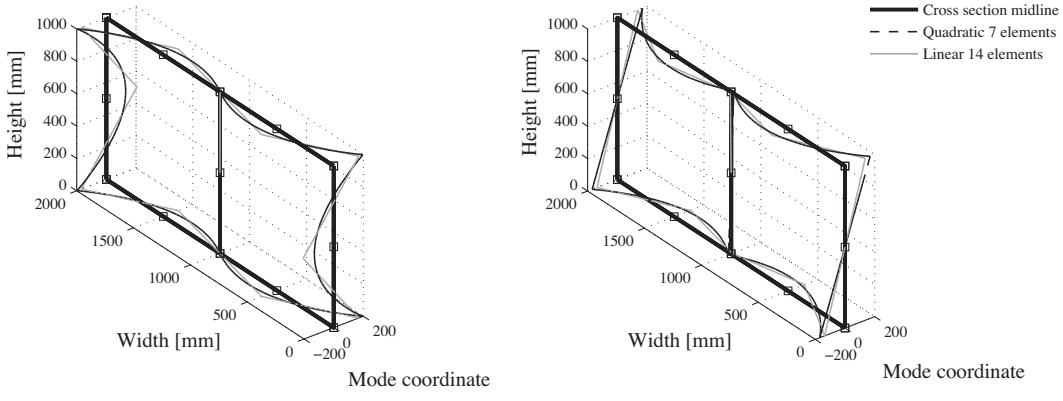

Fig. 5. Twin hollow section, shear lag warping modes.

Section 3. A concentrated load of $P = 10$ kN is applied at mid-span in one of the outer webs of the cross-section, as represented in Fig. 7, submitting the beam to a restrained torsion.

The finite element model implemented in [43] considers quadrilateral shell elements (S4), adopting a mesh of 28 elements along the beam cross-section and considering the span divided into 60 intervals, with a total of 1680 elements, which corresponds to 9882 degrees of freedom. The membrane axial stress distribution along the beam longitudinal axis obtained through the higher order beam mode herein developed and a shell model implemented in [43] is presented in Fig. 8. Nodal line A is relative to the top of the beam right web, whereas the nodal B represent the top of the beam left web.

A stress coloured map obtained using the developed model is represented in Figs. 9 and 10, where the effect of the local load can be observed. A comparison of the axial stresses distribution at the

Please cite this article in press as: Vieira RF et al. Definition of warping modes within the context of a higher order thin-walled beam model. Comput Struct (2014), http://dx.doi.org/10.1016/j.compstruc.2014.10.005

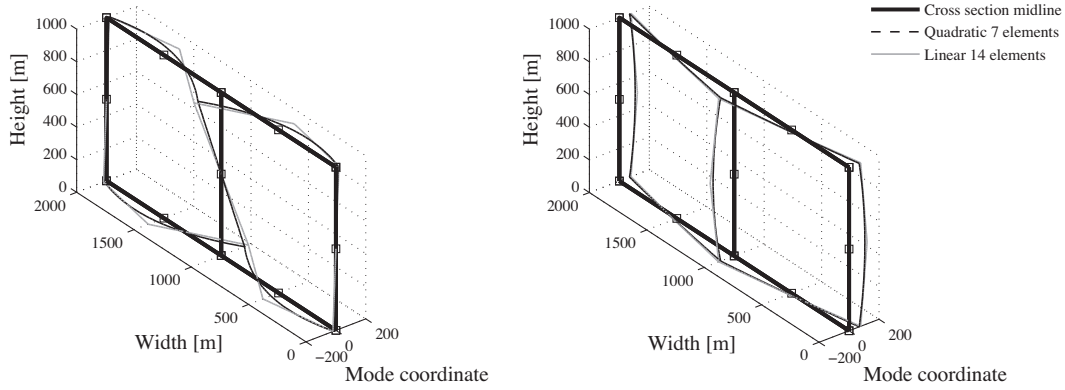

Fig. 6. Twin hollow section, higher order warping modes.

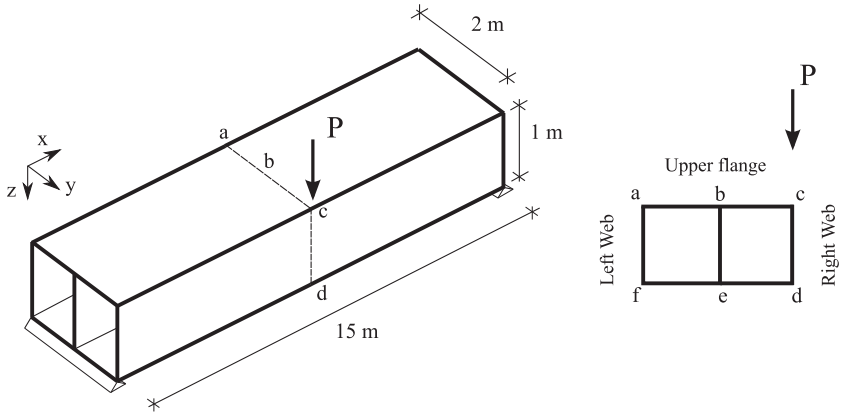

Fig. 7. Twin box beam loading.

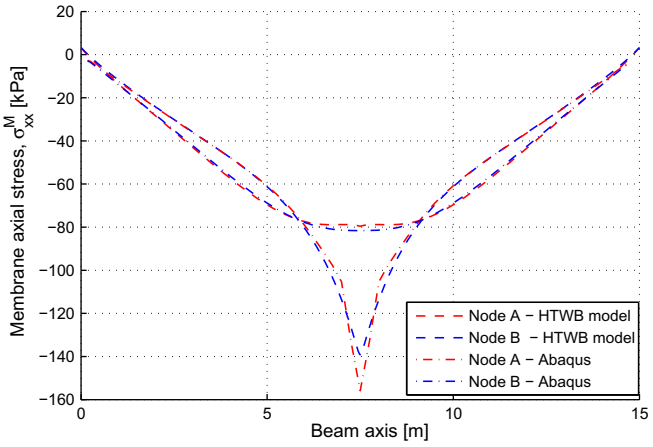

Fig. 8. Axial stress longitudinal distribution.

mid span cross-section obtained from the proposed model (green pentagrams), the model in [7] (blue pentagrams), the model in [19] (red pentagrams) and results obtained from the shell model using [43] (red circles) is presented in Fig. 11, being the corresponding stress values given in Table 1. A fairly good agreement of results exist, being the distribution of Sedlacek's the one which deviates more from the others.

An example from [35] that consists in a box girder cantilever with 10 m length subjected to an eccentric tip load of 1000 kN was considered so as to compare the model's performance regarding an alternative higher order beam theory. The geometry of the cantilever is depicted in Fig. 12 as well as the discretization adopted for the approximation of the displacement field over the cross-section. An elastic modulus of 40 GPa was adopted and the Poisson effect was neglected. Side by side, the cantilever was also analysed by a shell model implemented in [43] by adopting a mesh of quadrilateral shell elements (S4)(32 elements along the beam cross-section and considering the length divided into 40 intervals). Notice that the results obtained from the beam model of [35] correspond to an in-plane deformable cross-section.

The warping modes obtained from the developed model are depicted in Fig. 13 and represent meaningful structural behaviour, in that: (i) ω_1 is the first order warping mode associated with torsion, which corresponds to the classic warping defined by the sectorial coordinate, (ii) ω_2 is the second order warping mode associated with torsion and (iii) ω_3 the first higher order warping mode associated with flexure. This reasoning regarding each structural behaviour is underpinned by the eigenvalue solution of the model's equilibrium equation, having therefore both physical and mathematical consistency. It should be noticed that due to the fact of the closed cell being square, the cross-section warping associated with torsion (ω_1) does not involve the warping of the cell. Moreover, the derived warping modes are quite similar to the ones derived in [35] and depicted therein in appendix A.6.

Please cite this article in press as: Vieira RF et al. Definition of warping modes within the context of a higher order thin-walled beam model. Comput Struct (2014), http://dx.doi.org/10.1016/j.compstruc.2014.10.005

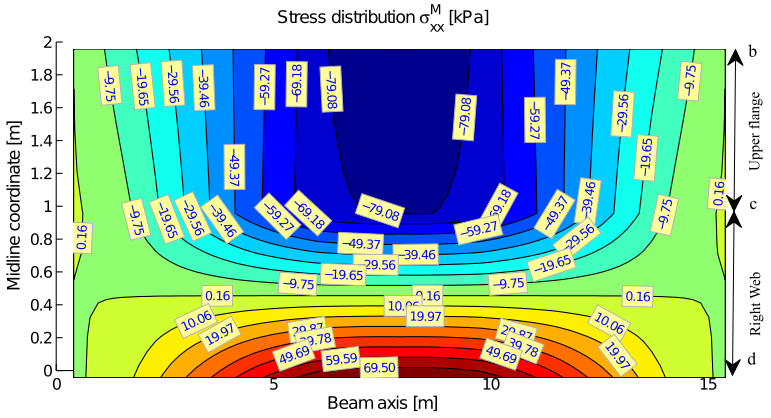

Fig. 9. Membrane axial stress [kPa], right web-upper flange.

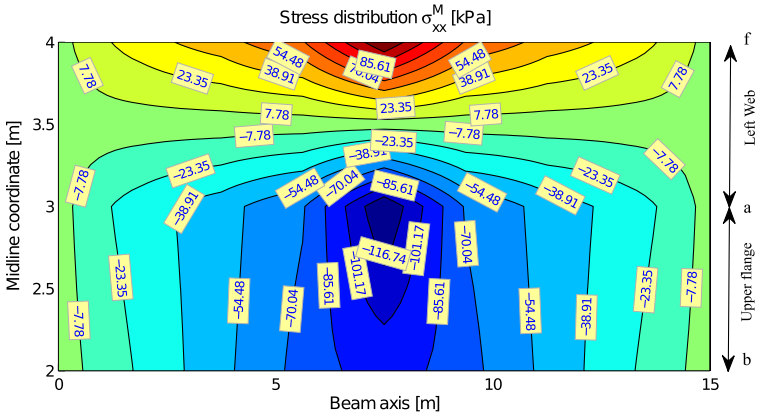

Fig. 10. Membrane axial stress [kPa], left web-upper flange.

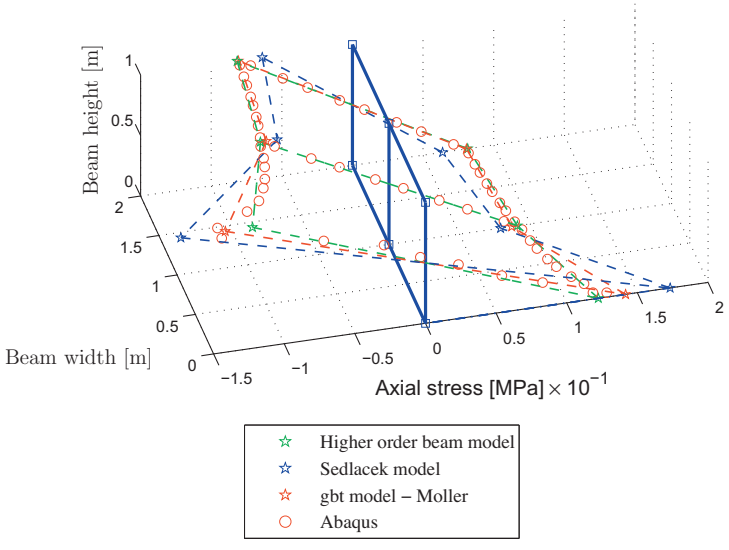

Fig. 11. Axial stress transverse distribution.

The axial stresses obtained from the developed higher order beam model at the upper flange of the box girder at $x = 0.05$ m (from the fixed end of the cantilever) are represented in Fig. 14. Two solutions of the higher beam model are represented: HOBM-a, which considers warping modes ω_1 to ω_3 and HOBM-b that considers all the higher order warping modes. The results obtained from [35] and from the shell model are also represented, being

Table 1
Axial stresses at mid-span [N/mm^2].

Model	c	b	a
Higher order beam model	−132.30	−88.99	−79.14
Sedlacek model	−173.20	−79.02	−63.80
GBT model (Moller)	−141.70	−86.91	−80.71
Abaqus	−129.60	−90.33	−80.76

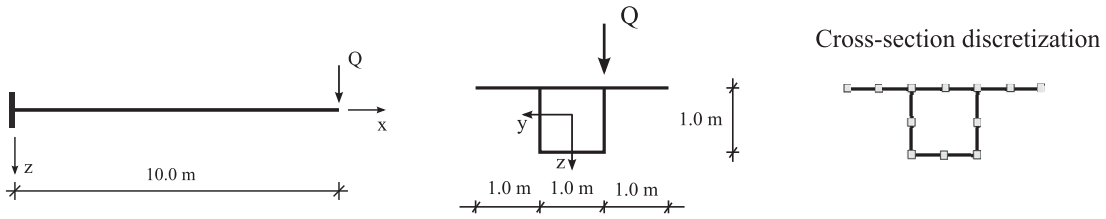

Fig. 12. Cantilever.

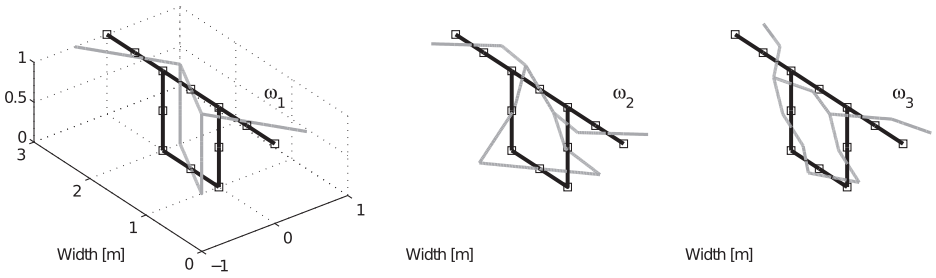

Fig. 13. Box girder warping modes.

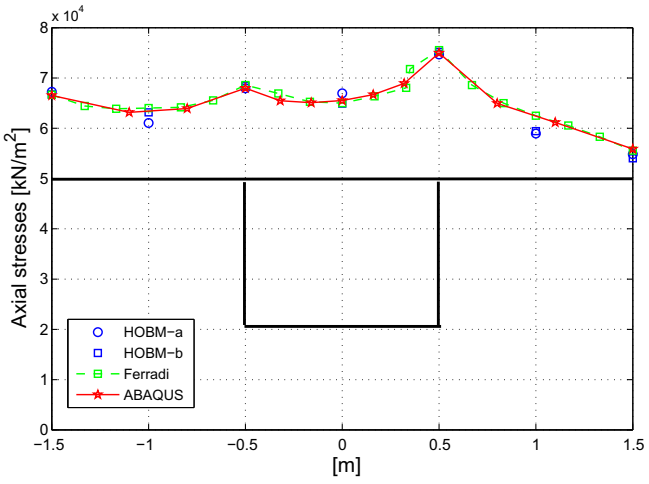

Fig. 14. Axial stresses at $x = 0.05$ m.

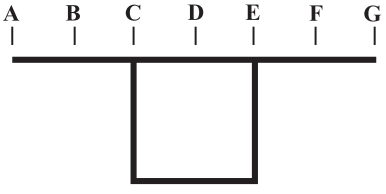

Fig. 15. Evaluation sections.

Table 2
Axial stresses at the built in end [N/mm^2].

Model	A	B	C	D	E	F	G
HOBM-a	67.28	61.06	67.97	66.97	74.70	58.97	54.84
HOBM-b	66.74	63.17	68.42	64.91	75.20	59.45	54.04
Ferradi model	66.67	64.03	68.61	65.00	75.55	60.55	55.56
Abaqus	66.53	63.17	67.98	65.53	74.98	61.17	55.89

verified a good agreement of results. The stress values of all models at the evaluation points identified in Fig. 15 are given in Table 2.

6. Conclusions

A beam model for the analysis of thin-walled beams was presented. The beam model relies on the approximation over the cross-section by a set of linear independent basis functions in order to properly capture the three-dimensional structural behaviour. The cross-section in-plane deformation is neglected, allowing to write the beam governing equations in terms of the axial components of the displacement field and establish a procedure for the uncoupling of the beam deformation modes through the corresponding generalised eigenvalue problem. A set of warping modes for some thin-walled cross-sections was hierarchically obtained by sorting the modes according to the respective eigenvalue. A twin-cell concrete girder simple supported was analysed considering the warping modes obtained, being the results successfully compared with (i) the results obtained through a shell finite element model implemented in [43] (where through kinematical constraints the cross-section was considered rigid), (ii) the results obtained by Sedlacek in [7] and (iii) the results obtained from the generalised beam theory formulation of Möller in [19]. Furthermore, a comparison with an alternative higher order beam theory presented in [35] was successfully presented.

References

[1] Vlassov V. Thin-walled elastic beams. Israel program for scientific translations Jerusalem; 1961.
[2] von Krmn T, Christensen N. Methods of analysis for torsion with variable twist. J Aeronaut Sci 1944;11:110–24.
[3] von Krmn T, Chien Z. Torsion with variable twist. J Aeronaut Sci 1949;16:451–62.
[4] Umansky. Bending and torsion of thin-walled aircraft constructions. Oborongiz, Moskow; 1939.
[5] Umansky. On normal stresses in torsion of an aircraft wing. Tekhnika vozdushnogo, Aircraft engineering; 1940.
[6] Benscoter S. A theory of torsion bending for multicell beams. J Appl Mech 1954.
[7] Sedlacek G. Systematische Darstellung des Biege- und Verdrehvorganges für prismatische Stäbe mit dünnwandigem Querschnitt unter Berücksichtigung der Profilverformung. PhD thesis, TU-Berlin; 1968.
[8] Sedlacek G. Zur berechnung der spannungsverteilung in dünnwandigen stäben unter berücksichtigung der profilverformungen. Der Stahlbau 1969.

Please cite this article in press as: Vieira RF et al. Definition of warping modes within the context of a higher order thin-walled beam model. Comput Struct (2014), http://dx.doi.org/10.1016/j.compstruc.2014.10.005

[9] Sedlacek G. Berechnung prismatischer faltwerke nach der erweiterten technischen biegetheorie. Der Bauingenieur 1971;46.
[10] Flugge, Marguerre. Wölbkrafte in dünnwandigen profilstäeben, warping in thin-walled beams. Ingenieur-Archiv 1948:23–38.
[11] Mavaddat S, Mirza M. Computer analysis of thin-walled concrete beams. Can J Civil Eng 1989;16:902–9.
[12] Razaqpur A, Li H. Thin-walled multicell box-girder finite element. J Struct Eng 1991;117:2953–71.
[13] Razaqpur A, Li H. Refined analysis of curved thin-walled multicell box-girder. Comput Struct 1994;53:131–42.
[14] Maisel B. Analysis of concrete box beams using small computer capacity. Cem Concr Assoc 1982.
[15] Roik K, Sedlacek G. Erweiterung der technischen biege-und verdrehtheorie unter berücksichtigung von schubverformungen. Die Bautechnik 1970;1:20–32.
[16] Schardt R. Eine erweiterung der technischen biegetheorie zur berechnung prismatischer faltwerke. Der Stahlbau 1966;35:161–71.
[17] Schardt R. Verallgemeinerte Technische Biegertheorie. Springer-Verlag; 1989.
[18] Schamckpfeffer H. Ermittlung der mittragenden Breite unter Bereucksichtigung von Längskraften, der Querträgerweichheit und in Längsrichtung verdnderlicher Querschnitte. PhD thesis, TU-Berlin; 1972.
[19] Möller R. Zur Berechnung prismatischer Strukturen mit beliebigem nicht formtreuem Querschnitt. PhD thesis, TU-Darmstadt; 1982.
[20] Simão F, Simões da Silva L. A unified energy formulation for the stability analysis of open and closed thin-walled members in the framework of the generalized beam theory. Thin-Wall Struct 2004;42:1495–517.
[21] Dinis P, Camotim D, Silvestre N. GBT formulation to analyse the buckling behaviour of thin-walled members with arbitrarily branched open cross-sections. Thin-Wall Struct 2004;44:20–38.
[22] Hanf H. Eine erweiterung der verallgemeinerten technischen biegetheorie zur erfassung von scheibenschubverzerrungen. Stahlbau 2011;79:114–25.
[23] Bauchau O. A beam theory for anisotropic materials. J Appl Mech 1980;52:416–22.
[24] Hjelmstad K. Warping effects in transverse bending of thin-walled beams. J Eng Mech 1987;113:907–24.
[25] Laudiero F, Savoia M. Shear strain effects in flexure and torsion of thin-walled beams with open or closed cross sections. Thin-Wall Struct 1990;10:87–119.
[26] Back S, Will K. A shear flexible element with warping for thin-walled open beams'. Int J Numer Methods Eng 1998;43:1173–91.
[27] Mentrasti L. Torsional stress concentration in thin-walled beams. J Eng Mech 1998;115:1882–903.
[28] Mentrasti L. Torsion of closed cross-section thin-walled beams: the influence of shearing strain. Thin-Wall Struct 1987;5:277–305.
[29] Prokic A. Thin-walled beams with open and closed cross-sections. Comput Struct 1993;47:1065–70.
[30] Prokic A. New warping function for thin-walled beams. i – Theory. J Struct Eng 1996;122:1437–41.
[31] Prokic A. New warping function for thin-walled beams. ii: Finite element method and applications. J Struct Eng 1996;122:1443–52.
[32] Prokic A. New finite element for analysis of shear lag. Comput Struct 2000;80:1011–24.
[33] Vieira RF, Virtuoso FB, Pereira EBR. A higher order thin-walled beam model including warping and shear modes. Int J Mech Sci 2013.
[34] Vieira RF, Virtuoso FB, Pereira EBR. Thin-walled structures: warping modes. In: Topping BHV, editor. Proceedings of the eleventh international conference on computational structures technology. Stirlingshire: Civil-Comp Press; 2012.
[35] Ferradi MK, Cespedes X. A new beam element with transversal and warping eigenmodes. Comput Struct 2014;131:12–33.
[36] Toupin R. Saint-Venant's principle. Arch Rational Mech Anal 1965;18:83–96.
[37] Flavin J. On knowles version of Saint-Venant's principle in two dimensional elastostatics. Arch Rational Mech Anal 1974;53:366–75.
[38] Knowles J. An energy estimate for the biharmonic equation and its application to Saint-Venant's principle in plane elastostatics. Indian J Pure Appl Math 1966;14:791–805.
[39] Goetschel D, Hu T. Quantification of Saint-Venant's principle for a general prismatic member. Comput Struct 1985;21:869–74.
[40] Goheberg I, Lancaster P, Rodman L. Matrix polynomials. SIAM; 1982.
[41] Braun M. Differential equations and their applications: an introduction to applied mathematics. Springer; 1993.
[42] Lancaster P, Webber P. Jordan chains for lambda matrices. Linear Algebra Its Appl 1968;1.
[43] ABAQUS. Standard Users Manual Version 6.8-1. SIMULIA Dassault Systmes; 2006.

Please cite this article in press as: Vieira RF et al. Definition of warping modes within the context of a higher order thin-walled beam model. Comput Struct (2014), http://dx.doi.org/10.1016/j.compstruc.2014.10.005